Bilad Alrafidain Journal for Engineering Science and Technology
https://doi.org/10.56990/bajest/2025.040103
ISSN: 2073-9524
Pages:22-34

Finite Element Analysis of Pre-stress Concrete Box-Girder under Thermal Loading

M. A. Ali[1**], A. H. Mohammed[2]
[1,2] Department of Civil Engineering, University of Diyala,32001, Iraq
engmohammedahmed059@gmail.com*[1], abbas_mohammed_eng@uodiyala.edu.iq[2]

Abstract
Bridge design and structural evaluation should consider thermal load, particularly for statically indeterminate and cable-supported bridges. However, there is limited study and test data on the thermal impact of pre-stress concrete girder, focusing on models developed through numerical analysis and field measurements. Temperature distributions on concrete bridges are nonlinear, causing stress distributions to self-equilibrate, to discuss the stresses, deflections, and moments caused by temperature variations. Three-dimensional finite element ANSYA R3 V19 finite element software is used to analyze pre-stress concrete box girder bridge specimens with trapezoidal cross sections. A parametric analysis was conducted to examine the effect of thermal loading on the behavior of prestressed concrete box girders. Six cases were considered to study the thermal behavior of the box girder. In each of these six cases, thermal loading was applied to three different regions of the box girder. The results showed that girder 3 and girder 6 with bottom thermal had the lowest deflected shape value of 0.84 mm when the thermal load was applied to the bottom flange of the prestressed concrete box girder, with reduced stresses observed in girder 2 and girder3 with top thermal, where the longitudinal stresses in the Z direction were 6.3 Mpa.

Keywords Finite Element, pre-stress, Concrete, Box-Girder, Thermal Loading, Analysis.

Article history: ***Received****: 06 Oct 2024;* ***Accepted****: 04 Nov 2024;* ***Published****: 15 Mar 2025*

1. Introduction

The box girder is a regularly used superstructure made up of two perpendicular or inclined webs intercommunicated by top and bottom slabs to form a single-cell or multi-cell box girder. The cross section of this construction is rectangular or trapezoidal. The box girder's cellular form is the consequence of eliminating unneeded materials, which reduces dead weight, hence lowering dead load and cost. The box girder has various advantages over the other sections, including better strength and torsional stiffness than the open section, a wider span range than the T-beam (resulting in fewer piers, and a more cost-effective design due to its hollow section [1].

The increase and decrease of temperatures are among the most critical factors influencing bridges. Temperature dissimilarities are influenced by the orientation of the structure, the material, the deck surface finishing toppings, the structure dimensions, and the cross-section geometries [2]. Bridges' performance is influenced by nonlinear heat load caused by these phenomena [3]. Organic glass modeling studies for box girders were carried out, and the experimental findings were compared to the finite element analytical results derived by MIDAS/Civil [4]. The creep and shrinkage of a box girder using an implanted vibration wire strain gauge.

* engmohammedahmed059@gmail.com

ISSN: 2073-9524
Pages:22-34

Mishra recently investigated the behavior of box girder bridges using the FEM and discovered it appropriate and beneficial in studying the box sections [5].

Based on Vlasov's thin-walled beam structural theory, I constructed the balancing differential equation of a double-symmetric box girder [6]. A temperature analysis technique was developed because of static loading testing on concrete box girder bridges [7]. The spatial FE technique was utilized to study the dynamic response of a thin-walled box girder bridge.

In the previous work of Zhang et al. [8], the authors focus on a fire that erupted on the Bill Williams River Bridge in Arizona, USA, which was made of pre-stressed concrete in 2006. The bridge featured fourteen spans with a total length of 23.2 meters and had a superstructure consisting of PC girders supporting a cast-in-place concrete slab. A similar destructive fire occurred in 2017 on the I-85 freeway in Iowa, where a pre-stressed concrete bridge collapsed after 40 minutes [8].

In this study, the ANSYS program is employed to develop model a FEM for the analyzing of pre stress concrete box girder under thermal loading. The goal is to examine the deformation and stress state of a concrete box girder under heat loading. In previous years, most studies concentrated on developing finite element analysis and tests on steel girders, with only a little study focusing on pre-stress concrete box girders. There have been almost no investigations on the thermal loads of pre-stress concrete box girder bridges.

2. Analytical work

2.1 Finite Element modeling

The concrete was modeled using an 8-node solid element known as Solid 65. The solid element contains 8 nodes, each having 3 degrees of freedom for translation in the nodal x, y, and z dimensions. The element may bend plastically, crack in three orthogonal directions, and crush. Fig. 1 shows the geometry and node positions for this element type.

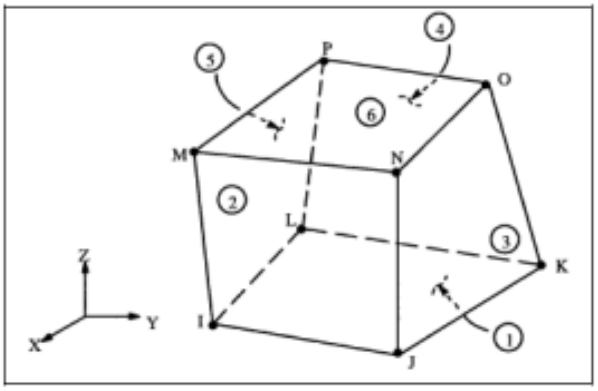

Fig. 1 Solid 65- 3D Reinforced concrete solid (ANSYS Help).

LINK180 is a spar (or truss) element that can be utilized in various engineering applications. This element is ideal for modeling trusses, sagging cables, linkages, springs, and similar structures. The 3-D spar element functions as a uniaxial tension-compression element with three degrees of freedom per node translations along the x, y, and z axes. As in a pin-jointed structure, element bending is not considered. It accounts for plasticity, creep, swelling, stress stiffening, and large deflections. In this study, the element was employed to simulate the pre-stressed tendons. Fig. 2 illustrates the LINK180 element.

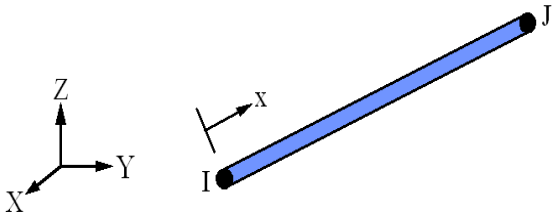

Fig. 2 Link 180 element (ANSYS Help) [9].

Steel plates are installed at the loading point to prevent stress concentration concerns. This results in a most uniform stress distribution over the load region. The steel plates were represented by (SHELL 181 in the software) as illustrated in Fig. 3.

ISSN: 2073-9524
Pages:22-34

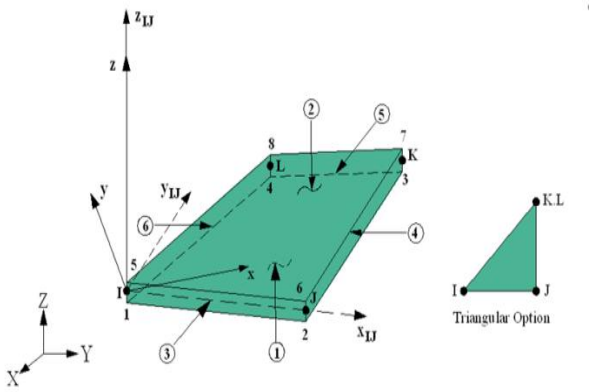

Fig. 3 SHELL 181 element (ANSYS Help) [10].

2.2 Geometry

To investigate the behavior of a standard pre-stressed concrete box girder bridge under thermal loads, a simply supported PC box girder was chosen for thermal performance analysis using ANSYS. The analysis included applying both structural loads and thermal effects to the girder. In this paper, the effect of thermal loading on PC box girders was studied. A thermal load of 50°C was applied only with temperature reference 25°C, without any structural load. The box girder, shown in Fig. 4, has a span length of 20000 mm and a sectional height of 1200 mm.

It is made up of one bottom flange, two webs, and one top flange, and simply supported ends. The top slab is 2400 mm wide and 180 mm thick, while the bottom slab is 1000 mm wide and 180 mm thick at the mid-span. The web is also 180 mm thick at the mid-span, with prestressing strands having an area of 139 mm²and417 mm². Additionally, both ends were restrained with iron plates, each 10 mm thick, to resist tensile forces resulting from the prestressing in the prestressed concrete box girder. The box girder is built of concrete with a cube strength of 30 MPa and pre-stressing strands with tensile strengths of 1395 and 1860 MPa. Fig. 5 depicts the details of the prestressing strands, including arrangement

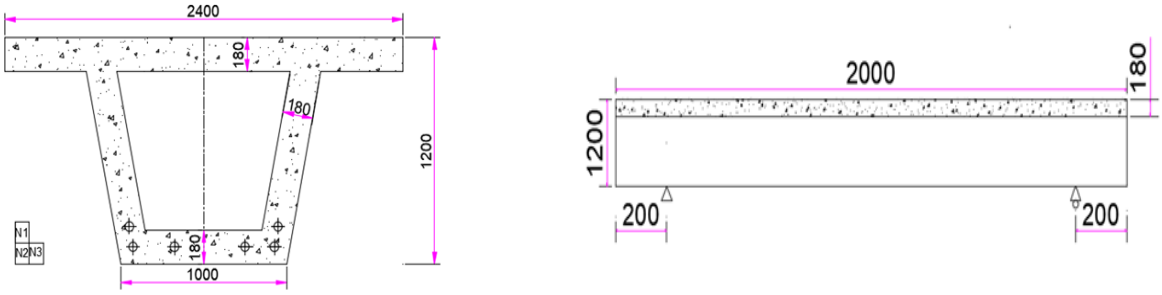

a) Cross section detail of girder at the mid-span. **b)** Simple Supported Prestressed Concrete Box.

Fig. 4 Pre-stress Concrete Girder (all dimensions are in mm).

For the thermal effect analysis, the selected pre-stressed concrete box girder was discretized using three types of components available in ANSYS SOLID65 for the concrete and SHELL181 for the steel plate, which was attached to both the right and left sides of the pre-stressed concrete box girder. SOLID65 elements were used to discretize the concrete portion of the PC box girder for structural analysis, while LINK180 elements simulated the prestressing strands.

To demonstrate the interaction between the concrete and the prestressing strands, adjacent nodes within the discretized girder were checked to establish connections between the solid concrete components and the prestressing strand link elements. The span ends feature multiline nodes on the lower surface of the bottom slab. Fig. 5 illustrates the modeling and meshing of the PC girder.

ISSN: 2073-9524
Pages:22-34

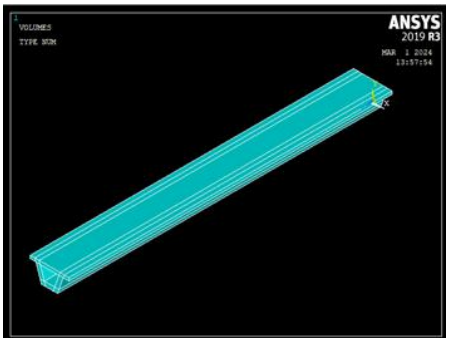

a) Modeling of PC box girder

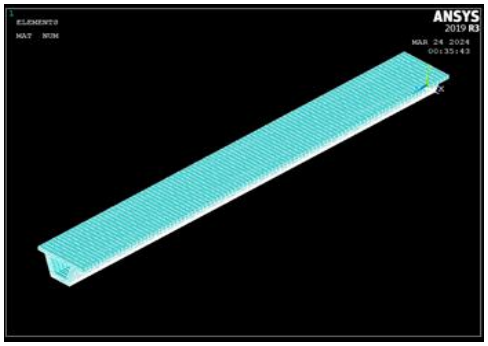

b) Meshing of PC box girder

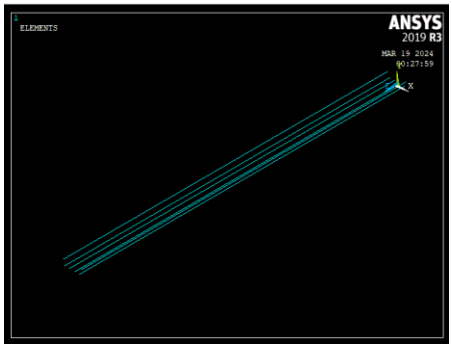

c. Meshing of prestressing strands No. 6

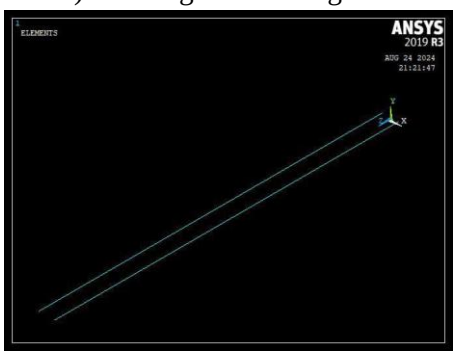

d) Meshing of prestressing strands No. 2

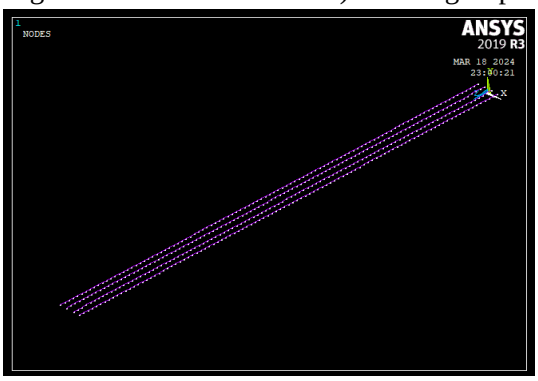

e) Meshing of prestressing strands No. 4

Fig. 5 Modeling meshing of prestressed concrete box girder.

To investigate the comportment of typical pre-stress concrete box girders below thermal loading conditions, a simply supported pre-stress concrete box girder was chosen to lead an analysis of thermal rendition using ANSYS by submitting it to thermal load exposure. This study comprises a nonlinear FE analysis for the PC box girders. The analysis was carried out by ANSYS software. Fig. 6 shows the cases considered for the parametric study.

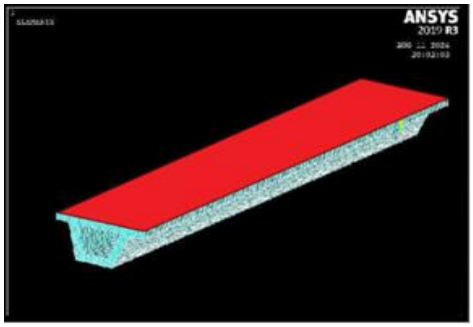

a) Thermal load at Top Flange.

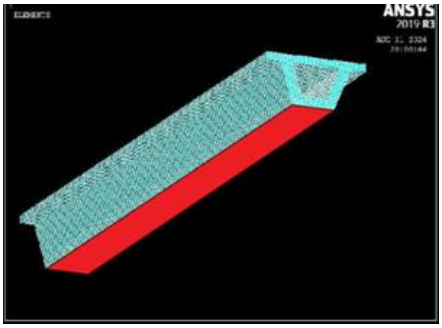

b) Thermal load at Bottom Flange.

ISSN: 2073-9524
Pages:22-34

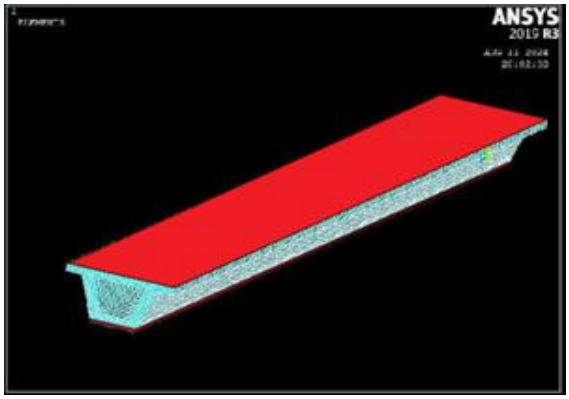

c) Thermal load at Top &Bottom flange.

Fig. 6 Location of applying thermal loading.

In this paper, the work has been divided into several cases based on the number of tendons, the area of the tendons, and the initial strength of the tendons. Additionally, the prestressed concrete box girder was subjected to thermal loading. The thermal load was applied to various regions of the prestressed concrete box girder.

3. Result and Discussion

Table 1 shows the variation in the interquartile range deflected shape and the number of stresses in the longitudinal direction (Z) in a pre-stressed box girder bridge exposed to thermal loading at a temperature of 50°C.

The interquartile range deviation in Girder 1 increased, reaching a maximum deflected shape of 6.5 mm when both the top and bottom flanges were exposed to thermal loading. The maximum stress in the longitudinal direction (Z) was 11.03 MPa when the bottom flange was exposed to thermal loading. This is primarily caused by thermal gradients, which result in thermal stresses and bending across the girder section.

In Girder 2, under exposure to heat (50°C), the interquartile range deflected shape gradually decreases to 1.7 mm due to the compression of the girder. This is mainly because the pre-stressed tendons can have a negative effect after the expansion of the concrete in both the top and bottom slabs, with the longitudinal stress (Z) decreasing to 6.3 MPa in the top slab.

In Girder 5, under thermal loading, the interquartile range deflected shape gradually increases, reaching 6.9 mm at its maximum when both the top and bottom slabs are exposed to thermal loading, with the longitudinal stress (Z) reaching 11.2 MPa.

This is mainly due to the deterioration of the concrete's strength and stiffness characteristics. In Girder 6, under thermal loading, the interquartile range deflected shape increases more rapidly, reaching 6.4 mm in the top flange, while the deflected shape decreases to 0.84 mm in the bottom flange, with longitudinal stresses increasing to 11.4 MPa. Table 1 presents the Result of the parametric study.

ISSN: 2073-9524
Pages:22-34

Table 1: Result of the parametric study

Girders	No. of tendons	Area of tendons (mm)	Initial strength (MPa)	Location of thermal loading	Deflected shape (mm)	Stress in Z direction (MPa)
Girder 1	6	139 = 834	1395	Top Flange.	2.8	9.04
				Bottom Flange.	3.7	11.03
				Top &Bottom flange.	6.5	10.7
Girder 2	4	139 = 556	1395	Top Flange.	2.59	6.3
				Bottom Flange.	4.4	11.6
				Top &Bottom flange.	1.7	9.3
Girder 3	2	139 = 278	1395	Top Flange.	2.6	6.3
				Bottom Flange.	0.84	10.4
				Top &Bottom flange.	1.7	8.5
Girder 4	6	417 = 2502	1860	Top Flange.	2.8	9.1
				Bottom Flange.	5.9	11.6
				Top &Bottom flange.	6.9	11.2
Girder 5	4	417 = 1668	1860	Top Flange.	2.8	9.1
				Bottom Flange.	3.8	9.8
				Top &Bottom flange.	6.9	11.2
Girder 6	2	417 = 834	1860	Top Flange.	6.4	9.8
				Bottom Flange.	0.84	11.4
				Top &Bottom flange.	1.7	9.2

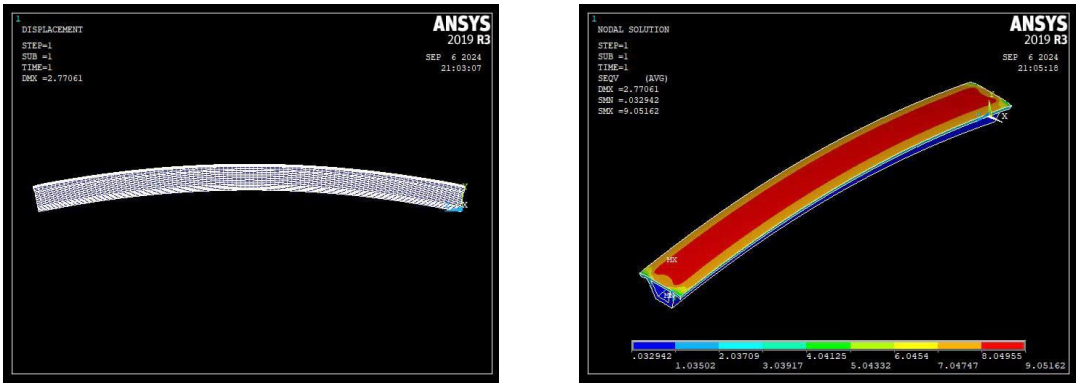

a) Deflected Shape b) Von Mises Stress

Fig. 7 For PC Box Girder1 with thermal load 50C˚ at top flange.

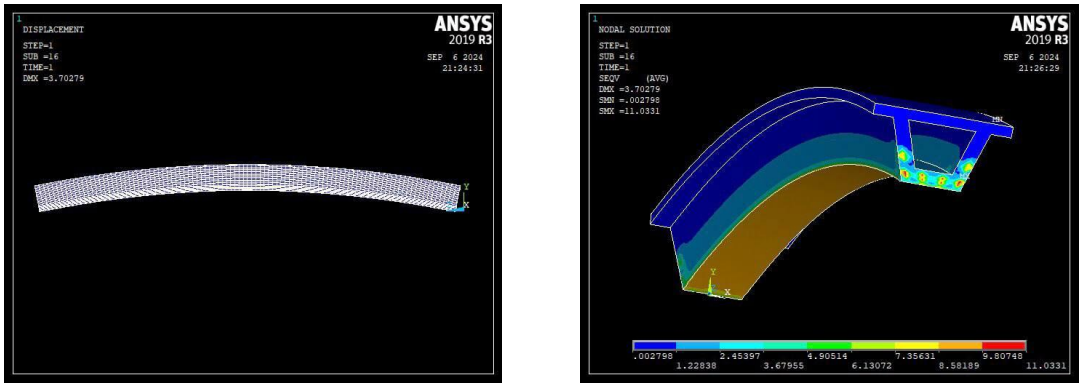

a) Deflected Shape b) Von Mises Stress

Fig. 8 For PC Box Girder 1 with thermal load 50C˚ at bottom flange.

ISSN: 2073-9524
Pages:22-34

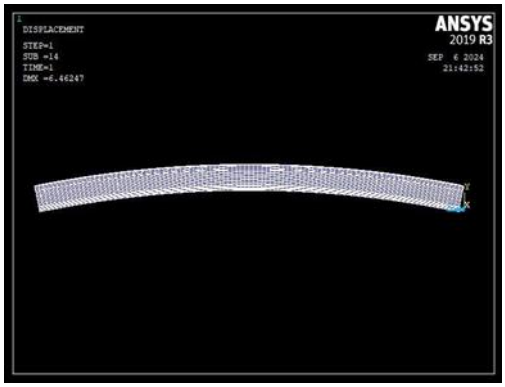

a) Deflected Shape

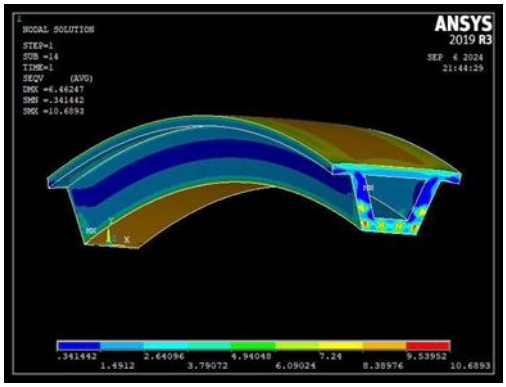

b) Von Mises Stress

Fig. 9 For PC Box Girder1 with thermal load 50C˚ at top and bottom flange.

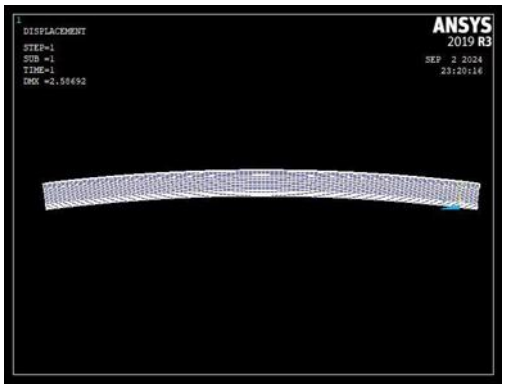

a) Deflected Shape

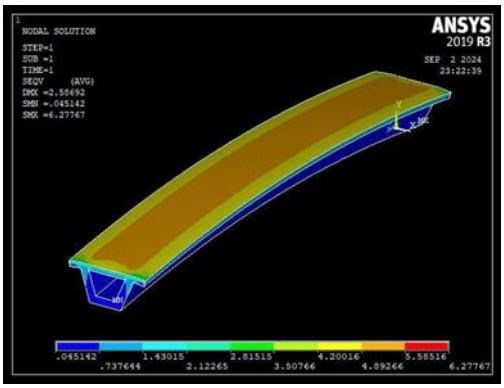

b) Von Mises Stress

Fig. 10 For PC Box Girder2 with thermal load 50C˚ at top flange.

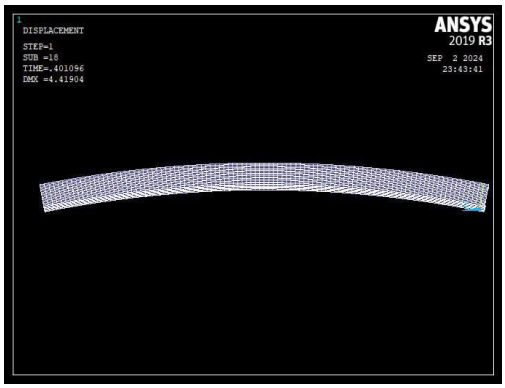

a) Deflected Shape

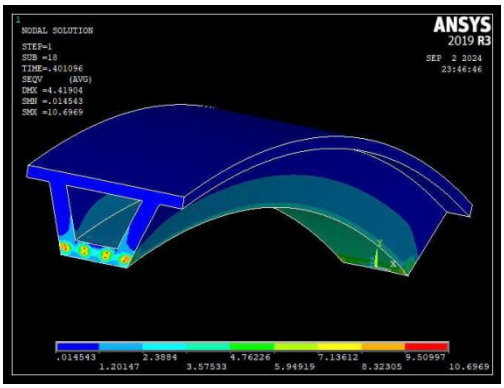

b) Von Mises Stress

Fig. 11 For PC Box Girder2 with thermal load 50C˚ at bottom flange.

ISSN: 2073-9524
Pages:22-34

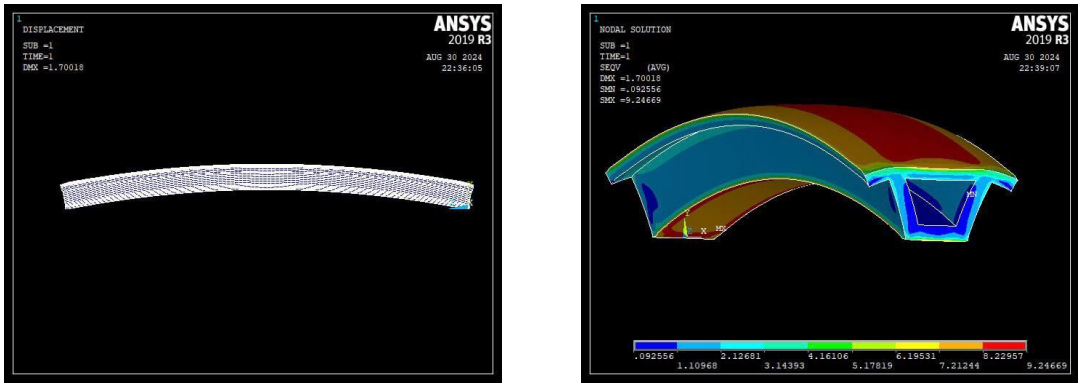

a) Deflected Shape b) Von Mises Stress

Fig. 12 For PC Box Girder2 with thermal load 50C˚ at top and bottom flange.

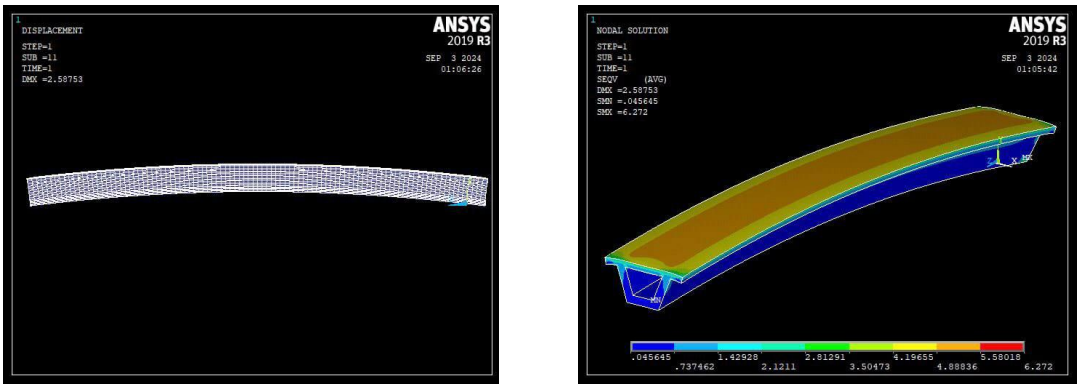

a) Deflected Shape b) Von Mises Stress

Fig. 13 For PC Box Girder3 with thermal load 50C˚ at top flange.

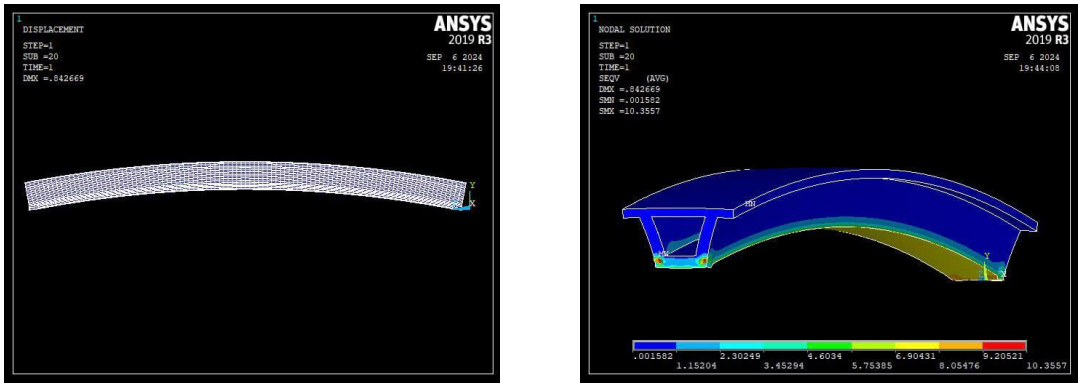

a) Deflected Shape b) Von Mises Stress

Fig. 14 For PC Box Girder3 with thermal load 50C˚ at bottom flange

ISSN: 2073-9524
Pages:22-34

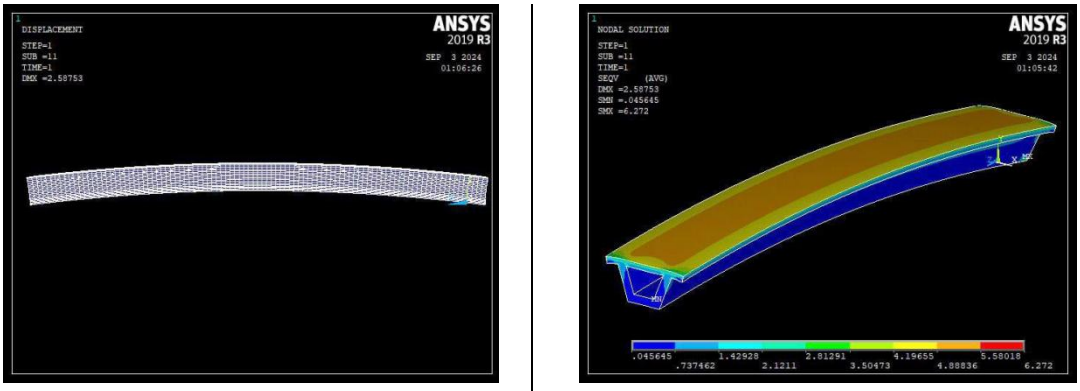

a) Deflected Shape b) Von Mises Stress

Fig. 15 For PC Box Girder3 with thermal load 50C˚ at top and bottom flange.

a) Deflected Shape b) Von Mises Stress

Fig. 16 For PC Box Girder 4 with thermal load 50C˚ at top flange

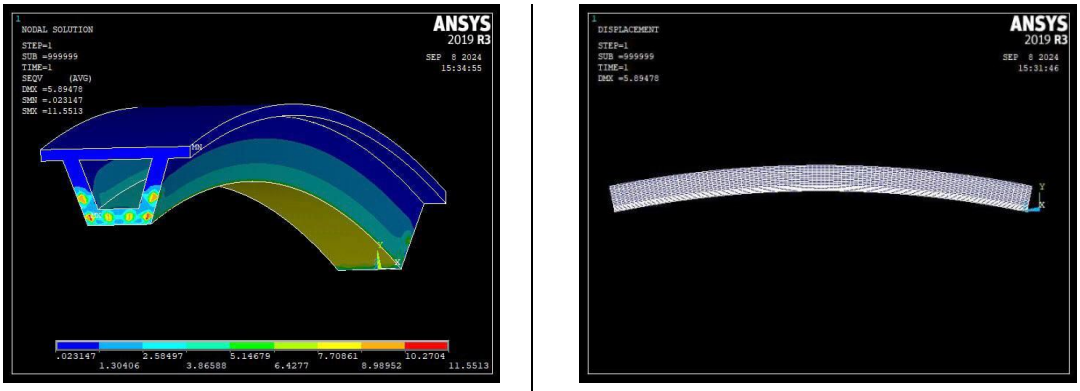

a) Deflected Shape b) Von Mises Stress

Fig. 17 For PC Box Girder 4 with thermal load 50C˚ at bottom flange

ISSN: 2073-9524
Pages:22-34

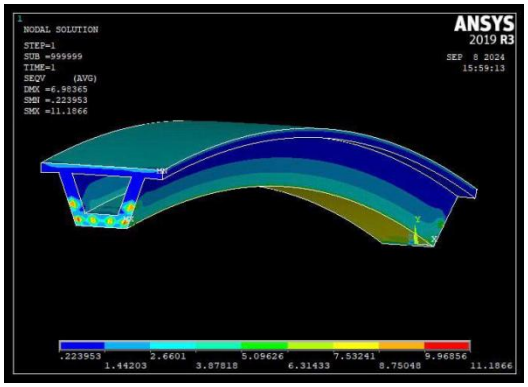

a) Deflected Shape

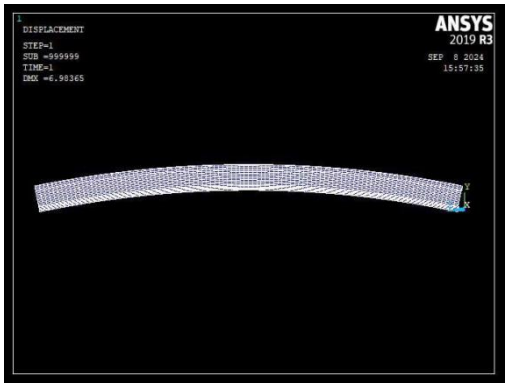

b) Von Mises Stress

Fig. 18 For PC Box Girder4 with thermal load 50C˚ at top and bottom flange.

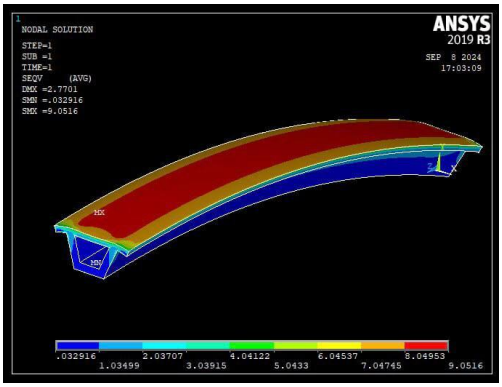

a) Deflected Shape

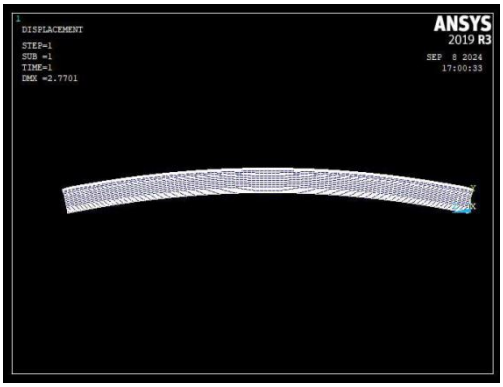

b) Von Mises Stress

Fig. 19 For PC Box Girder5 case-a- with thermal load 50C˚ at top flange

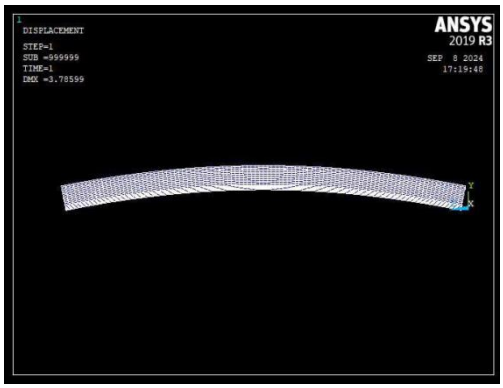

a) Deflected Shape

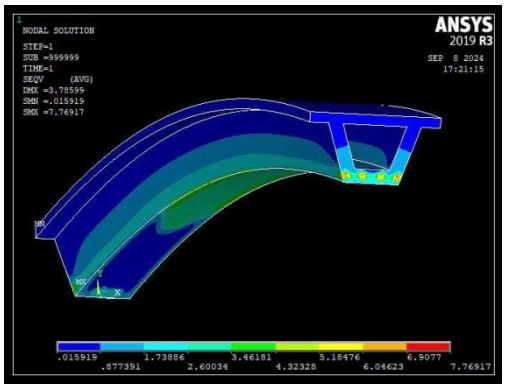

b) Von Mises Stress

Fig. 20 For PC Box Girder 5 with thermal load 50C˚ at bottom flange.

ISSN: 2073-9524
Pages:22-34

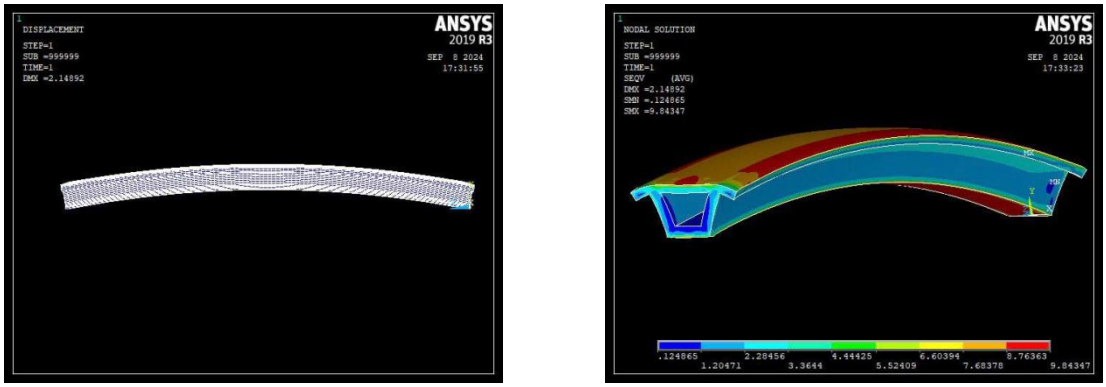

a) Deflected Shape b) Von Mises Stress

Fig. 21 For PC Box Girder 5 with thermal load 50C˚ at top and bottom flange.

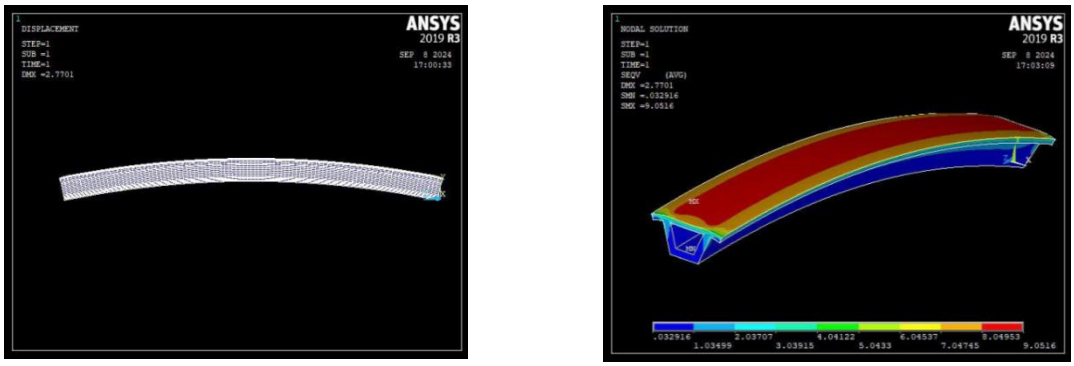

a) Deflected Shape b) Von Mises Stress

Fig. 22 For PC Box Girder 6 with thermal load 50C˚ at top flange

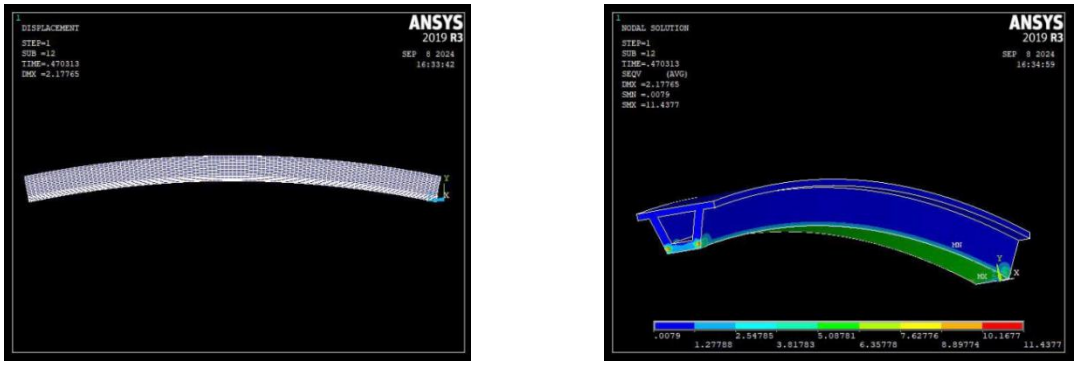

a) Deflected Shape b) Von Mises Stress

Fig. 23 For PC Box Girder 6 with thermal load 50C˚ at bottom flange

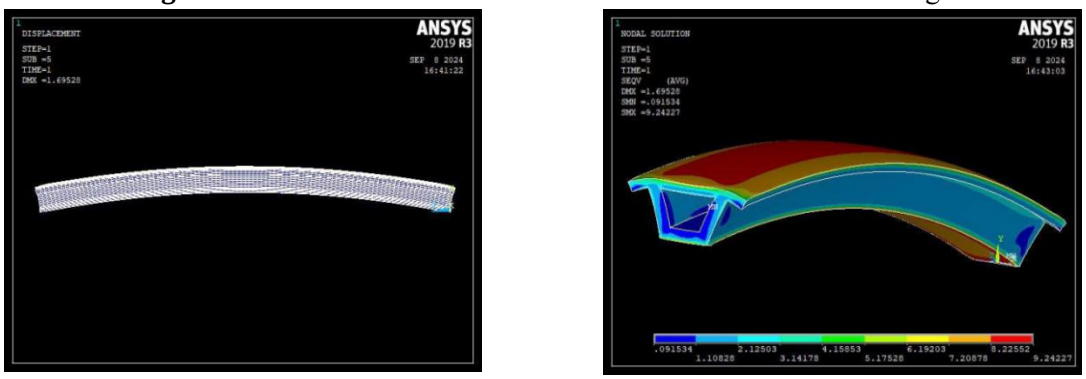

a) Deflected Shape b) Von Mises Stress

Fig. 24 For PC Box Girder6 with thermal load 50C˚ at top and bottom flange.

ISSN: 2073-9524
Pages:22-34

Figs. (7-24) shows the deflected shape and von Mises stresses for the prestress concrete box girder. The stresses in the top flange are tensile and uniform along the span. This is because the effect of thermal stresses is consistent along the span for the trapezoidal section. Since the web of the trapezoidal section is inclined, the thermal variation along the span is very slight and can be neglected. The change in stress distribution causes bending in the bridge, as the top flange of the box is more affected by heat than the bottom flange. As a result, the top flange expands more than the bottom flange. For the bottom flange, only compressive stresses occur due to the bending as well, Table 1 and Figures (7-24).

Fig. 7 shows in girder 1 the heat applied to the upper flange surface of the pre-stressed concrete box girder, where the numerical results showed the lowest amount of deflection at 2.8 mm compared to other cases for the same model. Fig. 21 shows Girder 5 interquartile range deflected shape steadily rises, reaching 6.9 mm at its maximum when both the top and bottom flanges are thermally loaded, with a longitudinal stress (Z) of 11.2 MPa. This is mostly due to the weakening of the concrete's strength and stiffness qualities.

Conclusion

The behavior of pre-stressed concrete box girders below heat stress was investigated using a transient nonlinear finite element technique. Prestressing has a major effect on thermal loads in prestressed concrete girders. Prestressed concrete box girders subjected to heat with higher prestressing deflect less than those with lesser prestressing.

1. For girder 1 and girder 4, tensile stresses occur on the upper edge and are evenly distributed across the span. This is because of thermal stresses; the fluctuation in the section's temperature over time is negligible and not considered. The numerical results in this case showed the highest deformation in girder 1 with top thermal, which amounts to 6.46 mm, and the highest stress value in girder 1 with bottom thermal, which is 11.03 MPa. Since heat affects the upper edge of the box more than the lower edge, the change in stress distribution will lead to a camber phenomenon in the bridge. As a result, the upper edge extends more than the lower edge.
2. In girder 2 and girder 5 of thermal exposure, the lowest deformation value of 1.7 mm occurs in girder 2 with thermal at the top and bottom flange, while the highest stress value of 9.8 MPa is observed in girder 5 with thermal at the top and bottom flange.
3. In girder 3 and girder 6 of thermal exposure, the lowest deformation value of 0.84 mm occurs in girder 3 with thermal at the bottom flange, while the highest stress value of 11.4 MPa is observed in girder 6 with thermal at the bottom flange.
4. When the top surface of the bridge is hotter than the bottom, the deflection is upward, and vice versa; when the top surface is less hot than the bottom, the deflection is downward.

Conflict of Interest

The authors declare that there are no conflicts of interest regarding the publication of this manuscript.

References

[1] Zahidi, Z.S. and Abbas, A.L. (2021) ‘Comparative Study of Structural Behaviour of Reinforced Concrete Box Girder with Different Numbers of Cells’, IOP Conference Series Materials Science and Engineering, 1076(1), p. 012110.

[2] Abod, R.N., Abdul-Razzaq, K.S. and Kadhum, A.K. (2024) ‘Pure Effect of Temperature on Rectangular and Trapezoidal Box-Girder Bridges – A Finite Element Investigation’, Diyala Journal of Engineering Sciences, 17(1), pp. 124–140. Available at https//doi.org/10.24237/djes.2024.17111.

[3] Zhao, Y., Zhou, Y., Feng, C., Liu, Z., & He, Z. (2016). Experimental and simulation analysis of prestressed concrete continuous box girder bridge. Rev. Tec. Ing. Univ. Zulia, 39, 392-398. Available at https//doi.org/10.21311/001.39.11.49.

[4] Ibrahim, N., Omenzetter, P. and Lipscombe, P. (2008) ‘Monitoring system for in-situ measurement of creep and shrinkage effects in a prestressed concrete bridge’, Futures in Mechanics of Structures and Materials - Proceedings of the 20th Australasian Conference

ISSN: 2073-9524
Pages:22-34

on the Mechanics of Structures and Materials, ACMSM20, (December 2008), pp.

[5] Chidolue, C.A. and Osadebe, N.N., 2012. Flexural torsional behaviour of thin-walled mono symmetric box girder structures. International Journal of Engineering Sciences and Emerging Technologies, 2(2), pp.11-19.

[6] Khadiranaikar, Dr RB, and Tiger Venkateshwar. "Effect of number of cells in psc box girder bridge." Development 3.6 (2016).

[7] Zhao, Y., Zhou, Y., Feng, C., Liu, Z., & He, Z. (2016). Experimental and simulation analysis of prestressed concrete continuous box girder bridge. Rev. Tec. Ing. Univ. Zulia, 39, 392-398.

[8] Zhang, G., Kodur, V., Xie, J., He, S. and Hou, W., 2017. Behavior of prestressed concrete box bridge girders under hydrocarbon fire condition. Procedia engineering, 210, pp.449-455.

[9] Ibrahim, A.M., Ali, N.K. and Salman, W.D. (2013) 'Finite element analysis of reinforced concrete slabs with spherical voids', Diyala Journal of Engineering Sciences, 6(4), pp. 15–37.

[10] Gupta, P.k. (2010) 'parametric study on behaviour of box-girder bridges using finite element method department', 11(1), pp. 135–148.